UAV-served Energy Harvesting-enabled M2M Networks for Green Industry-A Perspective of Energy Efficient Resource Management Scheme

Xiao-Ren Xu, Yi-Han Xu, Long Suo, Wen Zhou, *Member, IEEE,* Gang Yu, Arumugam Nallanathan, *Fellow, IEEE*

***Abstract*—As one of the most important metrics to sustainably provide communication services in green Industrial Internet of Things (IIoT), the problem of improving energy efficiency has constantly attracted extraordinary concerns from industry so far as to academia. In this paper, we intend to investigate the energy efficiency issue for an Energy Harvesting (EH)-enabled Machine-to-Machine (EH-M2M) communication underlaying Unmanned Aerial Vehicles (UAVs) networks from the perspective of resource management. Specifically, we are aiming at maximizing the average energy efficiency of EH-M2M communications by conjointly considering the EH time slot assignment, transmit power control and bandwidth allocation under the limitations of Quality of Service (QoS) and the available energy status of the EH-M2M devices. However, as the optimization problem is non-convex and NP-hard which is hard to tackle directly, we first transform the primitive objective function into a convex form equivalently by non-linear fractional programming and variable relaxation approach. After that, an iterative algorithm on the basis of Dinkelbach and Lagrangian theory is designed to optimize the resource management strategy. Finally, extensive simulation results demonstrate that the proposed scheme can establish more energy efficient communications compared to the benchmark schemes in different network settings.**

***Index Terms*—UAV communications, M2M communications, energy-harvesting, resource management, optimization**

I. Introduction

In the epoch of Industry 5.0, human-to-machine collaboration under the state of low source depletion is the innovative feature, the advanced Industrial Internet of Things (IIoT) system is jointly controlled by human brain and cyber-physical part, making the green manufactural process more productive and sustainable [1]. In order to satisfy the emerging requirements from industrial

This work was supported in part by National Natural Science Foundation of China under Grant of 61601275, College Student Science and Technology Innovation Foundation of Jiangsu Province in China under Grant of 202210298114Y and Introduction of high-level talents and overseas returnee's scientific fund in Nanjing Forestry University under Grant of GXL015.

Corresponding author: Yi-Han Xu

Xiao-Ren Xu is with the College of Information Science and Technology, Nanjing Forestry University, Nanjing 210037 China (e-mail: xiaorenxu@njfu.edu.cn).

Yi-Han Xu is with the College of Information Science and Technology, Nanjing Forestry University, Nanjing 210037 China and School of Electrical Engineering and Telecommunications, The University of New South Wales, Sydney 2052, Australia (e-mail: xuyihan@njfu.edu.cn).

Long Suo is with the College of Information Science and Technology, Nanjing Forestry University, Nanjing 210037 China (e-mail: lsuo@njfu.edu.cn).

Wen Zhou is with the College of Information Science and Technology, Nanjing Forestry University, Nanjing 210037 China (e-mail: wenzhou@ustc.edu).

Gang Yu is with the Department of Electronic and Electrical Engineering, The University of Sheffield, Sheffield S10 2TN, U.K. (e-mail: 1781895340@qq.com).

Arumugam Nallanathan is with the School of Electronic Engineering and Computer Science, Queen Mary University of London, London E1 4NS, U.K. (e-mail: a.nallanathan@qmul.ac.uk)

segment, Energy Harvesting-enabled Machine-to-Machine (EH-M2M) communications have been regarded as a promising enabler, drawing extensive concerns not only in industry but also in academia [2]. From the perspective of resource management, M2M Terminals (MTs) enable to reuse the resource of cellular networks to obtain direct communications mutually, which alleviates the burden of the base station and enhances the resource utilization for both cellular and Machine-Type Device (MTD) users [3-5]. However, it is also obvious that if the number of such type of MTD users is massive, mountainous power consumption will be generated, which results in a gordian challenge in IIoT. Thus, Energy Efficiency (EE) optimization is treated as a significant issue in investigating various industrial M2M communications. Noticeably, apart from the conventional ideas of promoting EE by taking methods to reduce energy consumption, the works of [6-8] proposed the EH technology to recharge MTs so that the EE of network can be enhanced, satisfying the requirements for green IoT in a further way. To replenish energy supplies for MTs, there are miscellaneous energy sources that can be utilized, such as wind, heat, solar, and electromagnetic wave [9]. In the work of [10], the authors improved the EE of cognitive M2M communications by means of harvesting the energy sources for M2M pairs from nearby Radio Frequency (RF) resources.

As a significant development orientation for the next industrial generation, EH-M2M communications demand a more flexible communication circumstance and a larger range of network coverage. But in this case, deploying traditional infrastructures to serve the machinery is difficult and costs too much. Concurrently, it also disobeys the crucial requirements of IIoT [11, 12]. Fortunately, Unmanned Aerial Vehicles (UAVs) have earned widespread concentrations because of their maneuverability and low power consumption which enable them to flexibly construct the network and reduce the cost in various scenarios [13]. Specifically, UAV is able to serve as an aerial platform in IIoT to serve ground equipments and enlarge network coverage, in such a way the devices in IIoT environment can communicate with less transmit power [14]. Different from traditional terrestrial base stations, the UAV can easily provide Line-of-Sight (LoS) propagations for ground users to enhance channel capacity [15]. Additionally, Device-to-Device (D2D) communications with the EH function underlaying UAV-assisted cellular networks have been well-investigated in literature [16, 17], in which the UAV-assisted D2D communication has been verified that it enables to improve the spectral efficiency and EE potentially and feasibly in Human-to-Human (H2H) communications. Motivated by this, UAV-assisted industrial M2M network has been considered as a key component in future industry 5.0. In order to get the utmost out of M2M and UAV communications and guarantee the Quality of Service (QoS), it is essential to program a robust resource management scheme.

A. Related Works

In this part, we retrospect numerous researches by predecessors that are relevant to the issues and enabling technologies for resource management in IIoT. In the next generation of industry, the IIoT network has higher demands for its greenness and reliability to support the human-to-machine cooperative automatic production, which is expected to improve the resource

utilization and reduce the consumption of communications while ensuring QoS. As a technology in great demand, wireless Cyber-Physical IIoT (CP-IIoT) networks have received widespread interests. The work of [18] investigated a CP-IIoT framework, which contains a central controller, multiple sensors and actuators to optimize the energy efficiency through resource management strategy in terms of transmit power allocation and channel assignment. Moreover, in the work of [19], the authors proposed a co-design framework of hierarchical transmission-estimation communication scheme to realize reliable transmission and accurate estimation for wireless control network under lower power consumption and computing burden, which prompts the network to adapt to the dynamic and complex IIoT situations. In particular, a multi-agents reinforcement learning-based scheme is proposed in [20] to handle the cooperation with task offloading and resource allocation problems in IIoT environment. In addition, in order to prolong the battery life and ensure the reliability of CP-IIoT, some pioneering studies [21-28] have conducted investigations on EH-enabled IIoT networks. Different from the former studies focusing on reducing the overload and consumption only through allocating resources, EH techniques supply the additional power for CP-IIoT system, enhancing the energy efficiency in an active way. In particular, the work of [21] comprehensively reviewed various EH-powered wireless network types, system architecture and critical design issues. The work of [22] studied the piezoelectric energy harvesting technology in IIoT machinery, a renewable method that can gather energy from ambient unused vibrations and convert it into electric energy to recharge devices is proposed. In [23], a wireless sensor node powered by harvested thermal energy is studied to monitor rotation machines. Some novel energy efficient protocols are presented in [24] for self-chargeable IIoT sensor networks, the authors analyse the protocol clusters in accordance with their power efficiency. Mission-critical ultra-Reliable Low Latency Communications (uRLLC) application based on EH-IIoT circumstance is investigated by [25], the authors proposed a self-defined transmission protocol to estimate the outage probability and block error rate. In the work of [26], a LoRa-based industrial network is studied, in which the wireless power transfer technology is utilized to decrease the energy consumption and recharge batteries to extend the lifespan of batteries by categorizing low transmit power level. In order to make full use of EH technologies in IIoT scenarios, a novel scheme is proposed in [27] to classify the knowledge for machinery in the area of EH based on the vital parameters and performance standards from existing techniques. In [28], an efficient energy trading model so-called energy blockchain can be extensively applied to tackle the safety and privacy issues in different IIoT scenarios. Based on the aforementioned, how to deal with the resource management problem such as time slot assignment, power control, etc when adopting the EH technology in industrial MTD connections scenario is regarded as a challenge since it is expected to jointly optimize the resource allocation for EH and transmission issues. Therefore, programming a robust resource management scheme combining the active technique and conservative method is of great urgency in future IIoT model.

Nevertheless, in the situation where IIoT terminals are massive or deployed in intricate environments, it is difficult for IIoT devices to obtain reliable communications. To tackle the challenge, UAV-served communication is commonly considered as a

prominent approach for its high mobility and flexible deployment [29-37]. In [29], the authors investigated the UAVs-assisted relaying mode for IoTs in a full-duplex state, which breaks the bottlenecks of the latency of IoT users and storage capacity of UAVs, respectively. In [30], a UAV-supported clustered non-orthogonal multiple access and wireless powered communication network is applied in 6G-enabled IoT network, in which an iterative algorithm owing to Lagrange Multiplier and bisection method is applied to significantly optimize the reachable sum rate on average. Authors in [31] developed a deep deterministic policy gradient algorithm facing multiple objections to maximize the sum rate and total harvested energy while minimizing the power consumption concurrently for a UAV-aided IoT network. In addition, the proposed algorithm has the capability of adjusting multi-objectives to cooperate with dynamic and uncertain environments. The work of [32] presented a Successive Convex Programming (SCP) method to maximize the total average data rate of ground nodes and applied for wireless power transfer and Orthogonal Frequency Division Multiplexing (OFDM) to address the energy supply and transmit path interference problems in UAV-powered IoT system. In [33], a generative adversarial long short-term memory network framework in UAV-served M2M communications has been proposed, the resource allocation issue is formulated to be a Markov game to evaluate the network performance and UAV mobility. The work of [34] investigated an innovative multi-attenuation channel model for 5G-UAV-assisted emergency wireless communications, the optimal transmission power and spectrum allocation method is proposed to establish an ultra-high capacity and energy efficient communication during the disaster rescue. Similarly, a resource allocation scheme for UAV-relay M2M communication in disaster zones to make rescue mission has been proposed in [35]. In [36], a reinforcement learning-based resource management that is suitable for multiple agents for UAV-aided communications has been presented to optimize joint power and bandwidth allocation. The long-term rewards of networks are optimized through Q-learning algorithm. Additionally, a robust resource allocation algorithm is designed in [37] to provide energy efficient communications for UAV-aided D2D networks in the case of optimal spectrum allocation and UAV flight coordinate. Moreover, energy efficiency is also considered as a significant issue in UAV-based networks with EH in recent studies. The work of [38] proposed a UAV-enabled EH communication system for users in half and full duplex, which focuses on the propulsion energy minimization of UAV while meeting the demands of minimal data transmission constraint, solved by SCP and one-dimensional search methods. In [39], multi-UAV relays between the source and IoT nodes assisted EH communication was presented, based on time switch and power splitting strategies. The outage probability and bit error rate are derived, and the authors analyze the throughput and delay limitation. However, to further realize the energy efficient communication for IIoT terminals, it is necessary to introduce EH-M2M communication underlaying UAV-assisted network scenario in the coming investigations as M2M is a momentous component in industrial automatic machinery networks.

B. Motivations and Contributions

Despite some researches that are on the cutting edge have worked out in different aspects of resource allocation in UAV-assisted

communications [40-42], EH-enabled communications [43-45] and the combined studies between the two areas [38-39], machinery network is hardly ever studied associated with the formers, especially for UAV-served EH-enabled Mechanical Arm (EH-MA) communication in industrial manufacturing process of this paper. Moreover, when focusing on the realistic EH-MA communication, energy efficiency is a critical problem. To achieve high energy efficiency and guaranteed QoS for EH-MA communication, it is necessary to investigate the influence from the perspective of resource management. Herein, combined with the advantages of resource allocation in UAV communication, it is of great value and more challenging to study the UAV-served EH-enabled M2M communications in IIoTs scenario. Motivated by the aforementioned, this paper investigates the energy efficient resource management for the UAV-served EH-M2M communication in IIoTs environment. Particularly, although [38-39] have studied the EE issue in UAV-based networks, M2M communication was not considered yet especially with the EH function. The main contributions in this work are summarized as follows.

- In this paper, we design a UAV-served EH-M2M communication framework. To construct a realistic IIoT network scenario, we intentionally consider the imperfect LoS propagation condition and the complex fading composition in the network model. We aim at maximizing the average EE for all the EH-M2M pairs while ensuring the QoS by formulating the resource management problem in terms of EH time slot and bandwidth allocation as well as controlling the transmit power.
- To cope with the mixed-integer non-linear optimization problem, we relax the variables and utilize nonlinear fractional programming theory to convert the fractional optimization function into a subtractive form equivalently. After that, the converted problem can be further transformed into a convex one with variable substitution. According to Dinkelbach and Lagrangian dual theory, an iterative algorithm jointly optimizing EH time slot assignment, bandwidth allocation and transmit power management is proposed to solve this formulated problem.
- Numerical results demonstrate that the optimal EE can be found using the proposed algorithm, which has a lower computational complexity than the benchmark schemes.

The rest of this paper is organized as follows. The UAV-served EH-M2M industrial network model is proposed in Section II. In Section III, we present the problem formulation and transform the original problem into a convex form. The iterative algorithm is designed in Section IV. Numerical results and performance analysis are both discussed in Section V. Finally, Section VI concludes this paper.

II. System Model

In this section, we in-depth present the system model of the multiple UAVs-served EH-enabled M2M communications in IIoT environment. TABLE I summarizes the main symbols that are referred to in this paper.

TABLE I

LIST OF MAIN SYMBOLS

Symbols	Description
$UAVs$	The set of UAVs
MAs	The set of MAs
K	The quantity of U2M channels
M	The quantity of EH-M2M channels
B_{sum}, B_{sub}	Sum available bandwidth and each orthogonal sub-bandwidth
X	The maximum number of EH-M2M pairs permitted to reuse the same U2M sub-bandwidth resource
$p_{i,k}^{(n)}$	Transmit power of the *i*-th UAV to *k*-th MA in time slot *n*
$p_{m,k}^{(n)}$	Transmit power between the *m*-th *MA_T* and *MA_R* on the *k*-th U2M sub-bandwidth in time slot *n*
$P_{m,n}$	Ergodic transmit power of the *m*-th EH-M2M pair in time slot *n*
P_{cir}	Static circuit power in MAs
$g_{i,k}^{(n)}$	Transmission channel gain between the *i*-th UAV and *k*-th MA in time slot *n*
$\tilde{g}_{i,k,m}^{(n)}$	Interference channel gain between the *i*-th UAV and the *m*-th *MA_R* on the *k*-th U2M sub-bandwidth in time slot *n*
$g_{m,k}^{(n)}$	Transmission channel gain between the *m*-th EH-M2M pair on the *k*-th U2M sub-bandwidth in time slot *n*

$\tilde{g}_{m,k}^{(n)}$	Interference channel gain between the *m*-th *MA_T* and *k*-th MA on the *k*-th U2M sub-bandwidth in time slot *n*
$\gamma_{i,k}^{(n)}$	SINR of the channel between the *i*-th UAV and *k*-th MA in time slot *n*
$\gamma_{m}^{(n)}$	SINR of the channel between the *m*-th EH-M2M pair in time slot *n*
$r_{i,k}^{(n)}$	Instantaneous industrial packet rate of the channel for U2M transmission mode in time slot *n*
$r_{m,k}^{(n)}$	Instantaneous industrial packet rate of the channel for EH-M2M transmission mode on the *k*-th U2M sub-bandwidth in time slot *n*
$R_{m,n}$	Ergodic industrial packet achievable rate of the *m*-th EH-M2M in time slot *n*
$R_{i,k}$	Minimum industrial packet transmission rate of each UAV-served MA
$EH_{m,n}$	Harvested energy flux at arrival time point t_n
$EE_{m,n}$	EE of the *m*-th EH-M2M in time slot *n*
EE_{M2M}	Average EE of all EH-M2M channels
E_0	Sum of the initial energy

In this paper, we consider a multiple UAVs-served EH-enabled M2M communication scenario in IIoT environment as illustrated in Fig. 1, which consists of a set of multi-antenna UAVs denoted as $UAVs = \{UAV_1,\ UAV_2, \dots, UAV_i, \dots, UAV_I,\}$ serving as aerial base stations and a set of single-antenna MAs denoted as $MAs = \{MA_1,\ MA_2, \dots, MA_l, \dots, MA_L\}$. Each MA is equipped with an EH facility to gather the ambient energy resources, then convert them into direct current energy. Via the power conditioning unit, the energy can be output to MA. All of the MAs are randomly deployed in a square area with the size of $R \times R$, thus the horizontal location of the *l*-th MA can be given by $u_l = [x_l, y_l]^T\ (\forall l \in \{1,2,\dots,L\}, \forall x_l, y_l < R)$. Besides, it is considered that *I* UAVs are flying in a straight route between the opposite vertexes of the $R \times R$ area, their two-dimension coordinates are expressed as $q_i = [x_i, y_i]^T\ (\forall i \in \{1,2,\dots,I\}, \forall x_i, y_i < R)$ and their flying altitude is fixed at H_I. In this way, we can take better advantage of the UAVs to expand the coverage of IIoT and guarantee the network QoS. In this network model, we assume that the sum available

bandwidth is B_{sum}, which is pre-allocated to UAVs and averagely divided into K orthogonal sub-bandwidths that is denoted as $B_{sub} = \left\{\frac{B_{sum}}{K}, \frac{2B_{sum}}{K}, \ldots, \frac{(K-2)B_{sum}}{K}, \frac{(K-1)B_{sum}}{K}, B_{sum}\right\}$ to provide the UAV-to-MA (U2M) links for ground MAs. However, the quantity of ground MAs is typically larger than the number of U2M sub-channels (i.e. $K < L$).

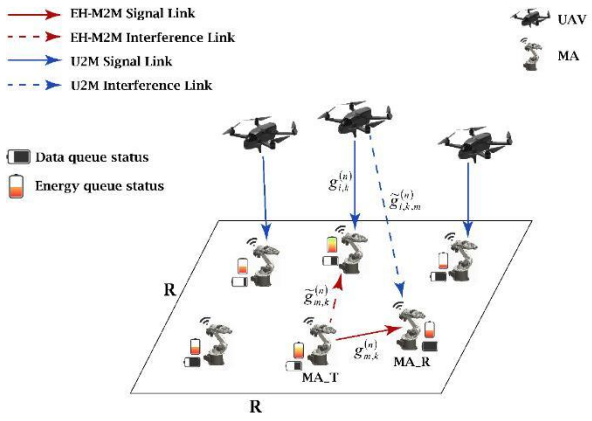

Fig. 1: Scenario of multiple UAVs-served EH-enabled M2M communications

For the purpose of making efficient use of the limited bandwidth resource, both U2M and M2M transmission modes are designed to support the data transmission in this network model. For the U2M transmission mode, K MAs are permitted to connect with UAVs and each MA antenna receives the industrial packets from one sub-channel. For the M2M transmission mode, M MA pairs are supposed to multiplex the pre-assigned UAV sub-bandwidths to establish the M2M communications, each M2M pair includes a MA transmitter (*MA_T*) and a MA receiver (*MA_R*). In this mode, the equipped EH-enabled facilities work towards harvesting the ambient energy to recharge the machinery. It's considered that all the energies used to maintain the M2M communications are provided by EH-enabled devices rather than factitious supply. Due to the uncertain environments and imperfect CSI, each MA enables to select its own transmission mode dynamically. Therefore, we regulate a binary indicator $o_{mk} \in \{0,1\}$ $(\forall m \in M, \forall k \in K)$ to denote whether the m-th EH-M2M pair occupies the k-th sub-bandwidth of the U2M transmission channel currently. To help with the investigation, time-slotted system is used in this model. For enhancing the efficiency of the resources in a further way, it is considered each sub-bandwidth of UAVs can be multiplexed by a maximum of X EH-M2M pairs within a time slot. Herein, one constraint should be satisfied as (1):

$$\sum_{m=1}^{M} o_{mk}^{(n)} \leq X, \quad \forall k \in K, n \in N \tag{1}$$

In the following, we discuss both of the channel models for U2M and EH-M2M transmission modes utilized in this industrial wireless machinery IoT scenario.

A. U2M Channel Model

Differentiate from conventional terrestrial communications, the proposed UAV-served MA communication model is regarded

as the Air-to-Ground (A2G) channel model, whose performance is highly subject to varying propagation environments. In this work, we denote a probabilistic path loss model for the U2M transmission channel that includes both the LoS and non-LoS (NLoS) propagation. The probability of LoS depends on the transmission environment, thus between UAV i and MA k in time slot n, it can be given by (2):

$$P_{i,k}^{LoS}(n) = \frac{1}{1 + a\, exp(-b\, sin^{-1}(\frac{h_{i,k}^{(n)}}{d_{i,k}^{(n)}}) - a)} \tag{2}$$

where a and b are constant values due to the ambient circumstance. $d_{i,k}^{(n)}$ and $h_{i,k}^{(n)}$ respectively denote the distance and relative height from the UAV i to MA k in time slot n. As for the U2M distance, the distance can be given by (3):

$$d_{i,k}^{(n)} = \sqrt{\left\| \overrightarrow{q_i^{(n)}} - \overrightarrow{u_k^{(n)}} \right\|^2 + h_{i,k}^{2(n)}} \tag{3}$$

where $\overrightarrow{q_i^{(n)}}$ and $\overrightarrow{u_k^{(n)}}$ denote the coordinates of UAV i and MA k in time slot n, respectively.

Therefore, the probability of establishing the NLoS links can be deduced as (4):

$$P_{i,k}^{NLoS}(n) = 1 - P_{i,k}^{LoS}(n) \tag{4}$$

Additionally, the path loss model for both LoS and NLoS propagations between the i-th UAV and k-th MA are expressed as (5a) and (5b):

$$L_{i,k}^{LoS}(n) = L_{i,k}^{FS}(n) + \eta^{LoS} \tag{5a}$$

$$L_{i,k}^{NLoS}(n) = L_{i,k}^{FS}(n) + \eta^{NLoS} \tag{5b}$$

where $L_{i,k}^{FS}(n)$ is the free space path loss, which is calculated by:

$$L_{i,k}^{FS}(n) = 20\, log(\, d_{i,k}^{(n)}) + 20\, log(\, f) + 20\, log(\frac{4\pi}{c}) \tag{6}$$

in which f denotes the carrier frequency and c denotes the velocity of light. The η^{LoS} and η^{NLoS} are the additive path losses for LoS and NLoS propagations.

Herein, considering the LoS and NLoS composition in propagation path loss, we categorized the ergodic U2M channel power gain between UAV i and MA k into $gL_{i,k}^{(n)}$ and $gN_{i,k}^{(n)}$ in time slot n respectively, which can be given by (7a) and (7b):

$$gL_{i,k}^{(n)} = \beta_0 d_{i,k}^{-\alpha L}(n) = \frac{\beta_0}{\left(\left\| \overrightarrow{q_i^{(n)}} - \overrightarrow{u_k^{(n)}} \right\|^2 + h_{i,k}^{2(n)} \right)^{-\frac{\alpha L}{2}}} \tag{7a}$$

$$gN_{i,k}^{(n)} = \mu\beta_0 d_{i,k}^{-\alpha N}(n) = \frac{\mu\beta_0}{\left(\left\| \overrightarrow{q_i^{(n)}} - \overrightarrow{u_k^{(n)}} \right\|^2 + h_{i,k}^{2(n)} \right)^{-\frac{\alpha N}{2}}} \tag{7b}$$

where β_0 is the mean channel gain between UAV and MA in unit distance (i.e. one meter), μ denotes the additive signal fading coefficient resulting from NLoS communication. In addition, αL and αN are the path loss exponents under the LoS and NLoS conditions.

From above discussion, the ergodic power gain in U2M channel model $g_{i,k}^{(n)}$ in time slot n can be calculated by (8):

$$g_{i,k}^{(n)} = P_{i,k}^{LoS}(n) \cdot gL_{i,k}^{(n)} + P_{i,k}^{NLoS}(n) \cdot gN_{i,k}^{(n)}, \quad \forall k \in K, n \in N \tag{8}$$

The interference in U2M channel derives from the reuse of the EH-M2M communications and the additive white Gaussian noise (AWGN) σ^2. Therefore, the instantaneous Signal-to-Interference plus Noise Ratio (SINR) of the U2M channel between the UAV i and MA k can be expressed as (9):

$$\gamma_{i,k}^{(n)} = \frac{p_{i,k}^{(n)} g_{i,k}^{(n)}}{\sum_{m=1}^{M} o_{mk}^{(n)} p_{m,k}^{(n)} \tilde{g}_{m,k}^{(n)} + \sigma^2}, \quad \forall k \in K, n \in N \tag{9}$$

where $p_{i,k}^{(n)}$ and $p_{m,k}^{(n)}$ respectively represent the transmit power of the i-th UAV and *MA_T* in the m-th EH-M2M pair reusing the k-th U2M sub-bandwidth in time slot n, and $\tilde{g}_{m,k}^{(n)}$ denotes the interference channel gain between the m-th *MA_T* and other MAs served by UAVs that reuses the same sub-channel pre-allocated to the UAV.

Therefore, based on the Shannon formula, the instantaneous industrial packet achievable rate between UAV i and MA k in time slot n is given by (10):

$$\begin{aligned} r_{i,k}^{(n)} &= B_{sub} \log_2\left(1 + \gamma_{i,k}^{(n)}\right) \\ &= B_{sub} \log_2\left(1 + \frac{p_{i,k}^{(n)} \cdot \left(P_{i,k}^{LoS}(n) \cdot \left(gL_{i,k}^{(n)} - gN_{i,k}^{(n)}\right) + gN_{i,k}^{(n)}\right)}{\sum_{m=1}^{M} o_{mk}^{(n)} p_{m,k}^{(n)} \tilde{g}_{m,k}^{(n)} + \sigma^2}\right) \end{aligned} \tag{10}$$

B. EH-M2M Channel Model

In this industrial machinery IoT system, partial MAs are grouped as MA pairs to obtain M2M communications by multiplexing the same bandwidth of the U2M channels. In this case, the MAs can harvest the energy sources from the ambient environment to sustain the M2M transmissions in an asynchronous mode. Because of the random energy input and reducing power loss, we consider the interval energy transfer for communication. Thus, $EH_{m,n}$ is denoted as the flux of harvested energy between time breath t_{n-1} and time breath t_n. Initialize $t_0 = 0$ and $t_n = T$ respectively, and the time-interval duration can be defined as $\tau_n = t_n - t_{n-1}$, where t_n and t_{n-1} are the energy achievable points in time. We model the achievable energy as a Poisson Process; therefore, the collected energy flux $EH_{m,n}$ at achievable time point t_n can be presented as (11):

$$EH_{m,n} \sim Poisson(\lambda \tau_n) \quad \forall m \in M, n \in N \tag{11}$$

where λ denotes the ergodic harvested energy per unit time (i.e. one second).

Particularly, both large-scale and small-scale fading are considered in this channel. We recognize the path loss and shadowing as the components of large-scale fading, which is denoted as $\chi_m$and ϑ_m, respectively. Meanwhile, the component of small-scale fading is the Rayleigh fading [46]. We denote $\zeta_m^{(n)}$ and $\zeta_m^{(n+1)}$ as the Rayleigh fading in time slot *n* and *n+1*, which can be given by (12):

$$\zeta_m^{(n+1)} = \rho\zeta_m^{(n)} + \sqrt{1-\rho^2}\delta \qquad (12)$$

where $\rho \in [0,1]$ is the relevancy indicator influencing the relevance of channel implementation into double successive blocks. Additionally, we denote δ and $\zeta_m^{(0)}$ as complex Gaussian random variables satisfying the distribution $CN(0,1)$.

In time slot *n*, the EH-M2M channel gain between *MA_T* and *MA_R* allocated by the *k*-th U2M sub-bandwidth can be given by (13):

$$g_{m,k}^{(n)} = \chi_m^{(n)} \cdot \vartheta_m^{(n)} \cdot \left|\zeta_m^{(n)}\right|^2 \qquad (13)$$

Then, the SINR of the EH-M2M transmission channel in time slot *n* is expressed as (14):

$$\gamma_m^{(n)} = \frac{p_{m,k}^{(n)} g_{m,k}^{(n)}}{o_{mk}^{(n)} p_{i,k}^{(n)} \tilde{g}_{i,k,m}^{(n)} + \sigma^2}, \quad \forall k \in K, m \in M, n \in N \qquad (14)$$

where $\tilde{g}_{i,k,m}^{(n)}$ denotes the interference channel gain between the UAV *i* and the *m*-th *MA_R* occupying the sub-bandwidth *k* from U2M channel in time slot *n*.

On the basis of Shannon formula, the instantaneous industrial packet achievable rate of the *m*-th EH-M2M channel reusing the *k*-th U2M sub-bandwidth in time slot *n* is calculated by (15):

$$r_{m,k}^{(n)} = B_{sub}\, log_2\left(1+\gamma_m^{(n)}\right)$$

$$= B_{sub}\, log_2\left(1 + \frac{p_{m,k}^{(n)} \cdot \chi_m^{(n)} \cdot \beta_m^{(n)} \cdot \left|\zeta_m^{(n)}\right|^2}{o_{mk}^{(n)} p_{i,k}^{(n)} \tilde{g}_{i,k,m}^{(n)} + \sigma^2}\right) \quad \forall k \in K, m \in M, n \in N \qquad (15)$$

Moreover, the ergodic industrial packet achievable rate of EH-M2M *m* in time slot *n* can be denoted as $R_{m,n}$, which can be written as:

$$R_{m,n} = \sum_{k=1}^{K} o_{mk}^{(n)} r_{m,k}^{(n)} \quad \forall m \in M, n \in N \qquad (16)$$

The ergodic transmit power in *m*-th EH-M2M pair in time slot *n* is denoted as $P_{m,n}$, which can be expressed as:

$$P_{m,n} = \sum_{k=1}^{K} o_{mk}^{(n)} p_{m,k}^{(n)} \quad \forall m \in M, n \in N \qquad (17)$$

III. Problem Formulation

A. Optimization Objective Function

In this section, we present the formulated cooperative optimization problem in terms of bandwidth and transmit power allocation as well as EH time slot assignment, while guaranteeing the energy harvesting robustness for all EH-M2Ms and the QoS in U2M channels. Our target is to maximize the average EE of all EH-M2M channels, and thus the EE of the m-th EH-M2M is denoted as $EE_{m,n}$ in time slot n, which can be calculated by:

$$EE_{m,n} = \frac{R_{m,n}}{\varepsilon P_{m,n} + P_{cir}} \quad \forall m \in M, \forall n \in N \tag{18}$$

where ε and P_{cir} are the inverse of efficiency for power amplifier and static circuit power, respectively. Herein, we present the average energy efficiency of total EH-M2M channels as EE_{M2M}, which can be calculated as (19):

$$EE_{M2M} = \sum_{n=1}^{N} \sum_{m=1}^{M} EE_{m,n} \tag{19}$$

In view of this, the maximization problem can be formulated by (20):

$$\max_{o_{mk}^{(n)}, p_{i,k}^{(n)}, p_{m,k}^{(n)}, t_{mk}^{(n)}} EE_{M2M} \tag{20}$$

subject to:

$$\sum_{m=1}^{M} o_{mk}^{(n)} \le X \quad \forall k \in K, n \in N \tag{20a}$$

$$\sum_{n=1}^{N} \sum_{k=1}^{K} o_{mk}^{(n)} p_{m,k}^{(n)} t_{mk}^{(n)} \le E_0 + \sum_{n=1}^{N} EH_{m,n} \quad \forall m \in M, n \in N \tag{20b}$$

$$\sum_{k=1}^{K} o_{mk}^{(n)} t_{mk}^{(n)} \le \tau_n \quad \forall m \in M, n \in N \tag{20c}$$

$$B_{sub} \log_2 \left(1 + \frac{p_{i,k}^{(n)} g_{i,k}^{(n)}}{\sum_{m=1}^{M} o_{mk}^{(n)} p_{m,k}^{(n)} \tilde{g}_{m,k}^{(n)} + \sigma^2} \right) \ge R_{i,k} \quad \forall k \in K, n \in N \tag{20d}$$

$$o_{mk}^{(n)} \in \{0,1\}, \quad p_{m,k}^{(n)} \ge 0, \quad 0 \le t_{mk}^{(n)} \le \tau_n, \quad p_{i,k}^{(n)} \ge 0 \tag{20e}$$

in which $(20a)$ is used to ensure that each sub-bandwidth resource of U2M channels can be multiplexed by at most X EH-M2M channels per time slot. $(20b)$ presents the energy limitation that the whole energy consumption is no more than the total amount of initial energy E_0 and total harvested energy over N time slots. $(20c)$ depicts the limited transmission duration, which implies that the EH-M2M transmission duration cannot exceed a period of time slot. $(20d)$ states the QoS limitation of the minimum industrial packet transmission rate of each UAV-served MA have to be over $R_{i,k}$.

B. Problem Equivalent Transformation

The problem (20) is a mixed-integer non-linear programming issue associated with a non-convex objective function and QoS limitations, which is a gordian challenge to tackle for the reason that the variables $t_{mk}^{(n)}$, $p_{m,k}^{(n)}$ and $p_{i,k}^{(n)}$ are consecutive while $o_{mk}^{(n)}$ is a binary variable. For the purpose of tackling this non-convex optimization problem, we first apply a function to represent the transmit power of U2M channels so as to transform the problem (20) into another equivalent one. It is assumed that the *m*-th EH-M2M enables to multiplex the *k*-th U2M sub-bandwidth resource in time slot *n* (i.e. $o_{mk}^{(n)} = 1$). According to $(20d)$, the transmit power in U2M channel can be written as (21):

$$p_{i,k}^{(n)} \geq \frac{\alpha\left(\sigma^2 + X p_{m,k}^{(n)} \tilde{g}_{m,k}^{(n)}\right)}{g_{i,k}^{(n)}}, \qquad (21)$$

where $\alpha = 2^{R_{i,k}/B_{sub}} - 1$.

For a fixed $p_{m,k}^{(n)}$, if $p_{i,k}^{(n)}$ increases, the function EE_{M2M} will decrease. Therefore, in order to deal with this uncertainty and reach the optimal energy efficiency EE_{M2M}^{*}, the optimal transmit power in U2M channel $p_{i,k}^{*(n)}$ should be given by (22):

$$p_{i,k}^{*(n)} = \frac{\alpha\left(\sigma^2 + X p_{m,k}^{(n)} \tilde{g}_{m,k}^{(n)}\right)}{g_{i,k}^{(n)}}, \qquad (22)$$

Next, we take the optimal transmit power $p_{i,k}^{*(n)}$ into optimization function (20a), it is proven to get the new optimization objective function (24). Denote$h_{mk}^{(n)}$, $e_{mk}^{(n)}$ and $f_{mk}^{(n)}$, which should satisfy (23):

$$\begin{cases} h_{mk}^{(n)} = g_{m,k}^{(n)} g_{i,k}^{(n)} \\ e_{mk}^{(n)} = g_{i,k}^{(n)} + \alpha \tilde{g}_{i,k,m}^{(n)} \\ f_{mk}^{(n)} = \alpha \tilde{g}_{m,k}^{(n)} \tilde{g}_{i,k,m}^{(n)} \end{cases} \qquad (23)$$

Herein, the primitive optimization problem (20) can be transformed as (24):

$$\max_{\ell} EE_{M2M} = \sum_{n=1}^{N} \sum_{m=1}^{M} \frac{\sum_{k=1}^{K} o_{mk}^{(n)} \log_2\left(1 + \frac{h_{mk}^{(n)} p_{m,k}^{(n)}}{e_{mk}^{(n)} \sigma^2 + f_{mk}^{(n)} p_{m,k}^{(n)}}\right)}{\varepsilon \sum_{k=1}^{K} o_{mk}^{(n)} p_{m,k}^{(n)} + P_{cir}} \qquad (24)$$

subject to

$$\sum_{m=1}^{M} o_{mk}^{(n)} \leq X \quad \forall k \in K, n \in N \qquad (24a)$$

$$\sum_{n=1}^{N} \sum_{k=1}^{K} o_{mk}^{(n)} p_{m,k}^{(n)} t_{mk}^{(n)} \leq E_0 + \sum_{n=1}^{N} EH_{m,n} \quad \forall m \in M, n \in N \qquad (24b)$$

$$\sum_{k=1}^{K} o_{mk}^{(n)} t_{mk}^{(n)} \leq \tau_n \quad \forall m \in M, n \in N \qquad (24c)$$

It is learned that the optimizing variables are updated to $\ell = \left\{o_{mk}^{(n)}, p_{m,k}^{(n)}, t_{mk}^{(n)}\right\}$ in (24). Thus, the optimized energy efficiency EE_{M2M}^{*} can be given by (25):

$$EE_{M2M}^{*} = max \sum_{n=1}^{N} \sum_{m=1}^{M} \frac{\sum_{k=1}^{K} o_{mk}^{*(n)} \, log_2\left(1 + \frac{h_{mk}^{(n)} p_{m,k}^{*(n)}}{\sigma^2 e_{mk}^{(n)} + f_{mk}^{(n)} p_{m,k}^{*(n)}}\right)}{\varepsilon \sum_{k=1}^{K} o_{mk}^{*(n)} p_{m,k}^{*(n)} + P_{cir}} \tag{25}$$

It is apparent that when each EH-M2M pair finds its optimal EE, the maximal average EE of the whole EH-M2M is EE_{M2M}^{*}, and vice versa. (The proof is given in **Appendix A**)

Therefore, the objective function can be updated as (26):

$$EE_{M2M}^{*} = \max_{\ell^*} \sum_{n=1}^{N} \sum_{m=1}^{M} EE_{m,n}^{*} \tag{26}$$

where the $EE_{m,n}^{*}$ can be presented as (27):

$$EE_{m,n}^{*} = \frac{\sum_{k=1}^{K} o_{mk}^{*(n)} \, log_2\left(1 + \frac{h_{mk}^{(n)} p_{m,k}^{*(n)}}{e_{mk}^{(n)} \sigma^2 + f_{mk}^{(n)} p_{m,k}^{*(n)}}\right)}{\varepsilon \sum_{k=1}^{K} o_{mk}^{(n)} p_{m,k}^{*(n)} + P_{cir}} \tag{27}$$

We denote

$$\begin{cases} R_{M2M}\left(o_{mk}^{*(n)}, p_{m,k}^{*(n)}\right) = \sum_{k=1}^{K} o_{mk}^{*(n)} \, log_2\left(1 + \frac{h_{mk}^{(n)} p_{m,k}^{*(n)}}{e_{mk}^{(n)} \sigma^2 + f_{mk}^{(n)} p_{m,k}^{*(n)}}\right) & (28) \\ P_{M2M}\left(p_{m,k}^{*(n)}\right) = \varepsilon \sum_{k=1}^{K} o_{mk}^{(n)} p_{m,k}^{*(n)} + P_{cir} & (29) \end{cases}$$

In this case, the fraction $EE_{m,n}^{*}$ can also be given as (30):

$$EE_{m,n}^{*} = \frac{R_{M2M}\left(o_{mk}^{*(n)}, p_{m,k}^{*(n)}\right)}{P_{M2M}\left(p_{m,k}^{*(n)}\right)} \tag{30}$$

In accordance with the non-linear fractional programming theory [47], we are supposed to transform the equation (30) into a corresponding subtractive form, which can be written as (31):

$$\begin{aligned} T1(\ell^*) &= \max_{\ell^*} \left(\sum_{k=1}^{K} o_{mk}^{*(n)} \, log_2\left(1 + \frac{h_{mk}^{(n)} p_{m,k}^{*(n)}}{e_{mk}^{(n)} \sigma^2 + f_{mk}^{(n)} p_{m,k}^{*(n)}}\right) - EE_{m,n}^{*} \left(\varepsilon \sum_{k=1}^{K} o_{mk}^{*(n)} p_{m,k}^{*(n)} + P_{cir} \right) \right) \\ &= \max_{\ell^*} \left(R_{M2M}\left(o_{mk}^{*(n)}, p_{m,k}^{*(n)}\right) - EE_{m,n}^{*} \left(P_{M2M}\left(p_{m,k}^{*(n)}\right) \right) \right) \end{aligned} \tag{31}$$

where $\ell^* = \left\{o_{mk}^{*(n)}, p_{m,k}^{*(n)}, t_{mk}^{*(n)}\right\}$.

On the basis of the non-linear fractional programming theory and the aforementioned, the optimization objective function (26) also should be converted into a corresponding subtractive form that can be rewritten as (32):

$$T2(\ell^*) = \max_{\ell^*} \sum_{n=1}^{N}\sum_{m=1}^{M}\left(\sum_{k=1}^{K} o_{mk}^{(n)} \log_2\left(+\frac{h_{mk}^{(n)} p_{m,k}^{*(n)}}{e_{mk}^{(n)}\sigma^2 + f_{mk}^{(n)} p_{m,k}^{*(n)}}\right) - EE_{m,n}^{*}\left(\varepsilon\sum_{k=1}^{K} o_{mk}^{*(n)} p_{m,k}^{*(n)} + P_{cir}\right)\right)$$

$$= \max_{\ell^*} \sum_{n=1}^{N}\sum_{m=1}^{M}\left(R_{M2M}\left(o_{mk}^{*(n)}, p_{m,k}^{*(n)}\right) - EE_{m,n}^{*}\left(P_{M2M}\left(p_{m,k}^{*(n)}\right)\right)\right) \quad (32)$$

It is obvious that when reaching the point $\left(p_{m,k}^{*(n)}, o_{mk}^{*(n)}\right)$ that is equal to (27) and (32), we can obtain the optimal $EE_{m,n}^{*}$. According to the Dinkelbach solving process [47] and Lagrangian limited optimization, the optimal $EE_{m,n}^{*}$ can be found.

Herein, the equivalent converted optimization function (24) has the following re-expression as (33):

$$\max_{\ell} \sum_{n=1}^{N}\sum_{m=1}^{M}\left(\sum_{k=1}^{K} o_{mk}^{(n)} \log_2\left(1+\frac{h_{mk}^{(n)} p_{m,k}^{(n)}}{e_{mk}^{(n)}\sigma^2 + f_{mk}^{(n)} p_{m,k}^{(n)}}\right) - EE_{m,n}\left(\varepsilon\sum_{k=1}^{K} o_{mk}^{(n)} p_{m,k}^{(n)} + P_{cir}\right)\right) \quad (33)$$

subject to:

$$\sum_{m=1}^{M} o_{mk}^{(n)} \le X \quad \forall k \in K, n \in N \quad (33a)$$

$$\sum_{n=1}^{N}\sum_{k=1}^{K} o_{mk}^{(n)} p_{m,k}^{(n)} t_{mk}^{(n)} \le E_0 + \sum_{n=1}^{N} EH_{m,n} \quad \forall m \in M, n \in N \quad (33b)$$

$$\sum_{k=1}^{K} o_{mk}^{(n)} t_{mk}^{(n)} \le \tau_n \quad \forall m \in M, n \in N \quad (33c)$$

It is verified that both $R_{M2M}\left(o_{mk}^{(n)}, p_{m,k}^{(n)}\right)$ and $P_{M2M}\left(o_{m,k}^{(n)}, p_{m,k}^{(n)}\right)$ are concave in $p_{m,k}^{(n)}$. (The proofs are provided in **Appendix B&C**)

The problem (33) is yet a non-convex problem and we believe it is NP-hard due to the integer variable $o_{mk}^{(n)}$. For the purpose of solving the problem, we relax $o_{mk}^{(n)}$ to interval $[0, 1]$. Meanwhile, we denote a variable $z_{mk}^{(n)} = o_{mk}^{(n)} p_{m,k}^{(n)}$ and transform the optimized function (33) into a manageable form. Replace $p_{m,k}^{(n)}$ by $\frac{z_{mk}^{(n)}}{o_{mk}^{(n)}}$, problem (33) can be rewritten as (34):

$$\max_{\ell} \sum_{n=1}^{N}\sum_{m=1}^{M}\left(\sum_{k=1}^{K} o_{mk}^{(n)} \log_2\left(1+\frac{h_{mk}^{(n)} \cdot \frac{z_{mk}^{(n)}}{o_{mk}^{(n)}}}{e_{mk}^{(n)}\sigma^2 + f_{mk}^{(n)} \cdot \frac{z_{mk}^{(n)}}{o_{mk}^{(n)}}}\right) - EE_{m,n}\left(\varepsilon\sum_{k=1}^{K} z_{mk}^{(n)} + P_{cir}\right)\right) \quad (34)$$

subject to:

$$\sum_{m=1}^{M} o_{mk}^{(n)} \le X \quad \forall k \in K, n \in N \quad (34a)$$

$$\sum_{n=1}^{N}\sum_{k=1}^{K} z_{mk}^{(n)} t_{mk}^{(n)} \le E_0 + \sum_{n=1}^{N} EH_{m,n} \quad \forall m \in M, n \in N \quad (34b)$$

$$\sum_{k=1}^{K} o_{mk}^{(n)} t_{mk}^{(n)} \le \tau_n \quad \forall m \in M, n \in N \qquad (34c)$$

The optimization objective function of the latest problem (34) is convex in $\left(o_{mk}^{(n)}, p_{m,k}^{(n)}\right)$. (The proof can be found in **Appendix D**)

Additionally, all the limitations in problem (34) are cooperatively convex in $o_{mk}^{(n)}$ and $z_{mk}^{(n)}$. Therefore, the transformed objective problem (34) is a convex optimization function.

IV. Proposed Optimal Algorithm

The problem (34) can be optimally and effectively tackled under the Karush-Kuhn-Tucker (KKT) conditions since this optimization objective function is convex. We relax the constraints in $(33a)$, $(33b)$ and $(33c)$, then propose the Lagrangianas:

$$\begin{aligned} L(\ell, \Psi) = &- \sum_{n=1}^{N}\sum_{m=1}^{M}\sum_{k=1}^{K} o_{mk}^{(n)} \log_2\left(1 + \frac{h_{mk}^{(n)} p_{m,k}^{(n)}}{e_{mk}^{(n)}\sigma^2 + f_{mk}^{(n)} p_{m,k}^{(n)}}\right) - EE_{M2M}\left[\varepsilon \sum_{n=1}^{N}\sum_{m=1}^{M}\sum_{k=1}^{K} o_{mk}^{(n)} p_{m,k}^{(n)} + P_{cir}\right] \\ &+ \sum_{n=1}^{N}\sum_{k=1}^{K} \lambda_{1,k,n}\left(\sum_{m=1}^{M} o_{mk}^{(n)} - X\right) + \sum_{n=1}^{N}\sum_{m=1}^{M} \lambda_{2,m,n}\left(\sum_{n=1}^{N}\sum_{k=1}^{K} o_{mk}^{(n)} p_{m,k}^{(n)} t_{mk}^{(n)} - E_0 - \sum_{n=0}^{N-1} EH_{m,n}\right) \\ &+ \sum_{n=1}^{N}\sum_{m=1}^{M} \lambda_{3,m,n}\left(\sum_{k=1}^{K} o_{mk}^{(n)} t_{mk}^{(n)} - \tau_n\right) \qquad (35) \end{aligned}$$

where we denote $\lambda_{1,k,n} \ge 0, \lambda_{2,m,n} \ge 0, \lambda_{3,m,n} \ge 0$as the Lagrangian multipliers that parallel to the limitations in (33a), (33b) and (33c), respectively. Moreover, the dual function can be defined as (36):

$$g(\Psi) = \max_{\ell} L(\ell, \Psi), \qquad (36)$$

where $\ell = \left\{o_{mk}^{(n)}, p_{m,k}^{(n)}, t_{mk}^{(n)}\right\}$ and $\Psi = \left(\lambda_{1,k,n}, \lambda_{2,m,n}, \lambda_{3,m,n}\right)$.

It is considered that the bandwidth resource in the *k*-th U2M sub-bandwidth is assigned to the *m*-th EH-M2M channel. Thereby, the optimized transmit power and transmission time $p_{m,k}^{*(n)}$ and $t_{mk}^{*(n)}$ can be reasoned respectively as (37) and (38):

$$p_{m,k}^{*(n)} = max\left\{0, \frac{\lambda_{3,m,n}}{\lambda_{2,m,n}}\right\} \qquad (37)$$

$$t_{mk}^{*(n)} = -\frac{e_{mk}^{(n)} h_{mk}^{(n)} \sigma^2}{\lambda_{2,m,n}\, ln\, 2\left(e_{mk}^{(n)}\sigma^2 + p_{m,k}^{(n)} \cdot \left(f_{mk}^{(n)} + h_{mk}^{(n)}\right)\right) \cdot \left(e_{mk}^{(n)}\sigma^2 + f_{mk}^{(n)} p_{m,k}^{(n)}\right)} + \frac{\varepsilon EE_{m,n}}{\lambda_{2,m,n}} \qquad (38)$$

Furthermore, we find the dual function (36) enables it to be decoupled into *K* separate sub-problems, which relates to *k*-th sub-bandwidth resource is as (39):

$$\max_{\ell_k} L_k(\ell_k, \Psi), \qquad (39)$$

where $\ell_k = \left\{o_k^{(n)}, p_k^{(n)}, t_k^{(n)}\right\}$. We denote $o_k^{(n)}$, $p_k^{(n)}$ and $t_k^{(n)}$ as the k-th column of o, p, t matrices, which are at the k-th sub-bandwidth resource in time slot n.

Owing to the constraint (34a), one sub-bandwidth resource in single U2M channel can be assigned to X EH-M2M transmission pairs, and the indicator $o_k^{(n)}$ of bandwidth resource is a matrix only including zero and no more than X non-zero entry. Herein, the optimal indicator $o_{mk}^{*(n)}$ can be deduced in:

$$o_{mk}^{*(n)} = \begin{cases} 1, & k = \underset{1 \le k \le K}{argmax} \eta_{m,k}^{(n)} \\ 0, & otherwise \end{cases} \qquad (40)$$

in which we can obtain:

$$\eta_{m,k}^{(n)} = -log_2\left(1 + \frac{h_{mk}^{(n)} g_{m,k}^{(n)}}{e_{mk}^{(n)}\sigma^2 + f_{mk}^{(n)} p_{m,k}^{(n)}}\right) \qquad (41)$$

From (40), it is obvious to see that the value $\eta_{m,k}^{(n)}$ is optimal when the k-th sub-bandwidth resource can be assigned to the m-th EH-M2M in time slot n. Besides, from (41), it is obvious that different channel gains have decisive impacts on the $\eta_{m,k}^{(n)}$. In consequence, we can get an integer solution from the temporary relaxation of $o_{mk}^{(n)}$ within [0, 1] and propose an iterative algorithm to optimize the EE of EH-M2M channels in terms of the energy-harvesting time slot assignment, bandwidth allocation and transmit power management in Algorithm 1.

Algorithm 1:

1. Input: $R_{i,k}, g_{i,k}, \forall k; g_{m,k}, \tilde{g}_{i,k,m}, \forall k, m; EH_{m,n}, \forall m, n; \tau_n, \forall n,$

2. T_{opm}, N, M, K, σ^2, α

3. Output: $p_{m,k}^{*(n)}, t_{m,k}^{*(n)}, o_{mk}^{*(n)}, p_{i,k}^{*(n)}, \forall k, m, n; \eta_{ee}^*$

4. Initialize η_{ee} point and maximal tolerance ε

5. Initialize $\lambda_{2,m,n}^{(0)} = 1$ and $\lambda_{3,m,n}^{(0)} = 1$

6. Calculate $p_{m,k}^{*(n)}$ and $t_{mk}^{*(n)}$, $\forall m, k, n$, with the obtained $\lambda_{2,m,n}$, $\lambda_{3,m,n}$ from (37) and (38)

7. Calculate $\eta_{m,k}^{(n)}, \forall m, k, n$ from (41)

8. Match the m-th EH-M2M channel with k-th sub-bandwidth resource from (40)

9. **while** $T2(\ell) > \varepsilon$, **do**

10. $\lambda_{2,m,n}^{(\theta+1)} = \left(\lambda_{2,m,n}^{(\theta)} - \alpha\left(\sum_{n=0}^{N-1} EH_{m,n} - \sum_{n=1}^{N}\sum_{k=1}^{K} o_{mk}^{(n)} p_{m,k}^{(n)} t_{mk}^{(n)}\right)\right)^+$

11. $\lambda_{3,m,n}^{(\theta+1)} = \left(\lambda_{3,m,n}^{(\theta)} - \beta\left(\tau_n - \sum_{k=1}^{K} o_{mk}^{(n)} t_{mk}^{(n)}\right)\right)^+$

12. Calculate $p_{m,k}^{(n)}, t_{mk}^{(n)}, o_{mk}^{(n)}, \eta_{ee}$

13. **end while**

14. obtain $p_{i,k}^{*(n)} = \frac{\alpha\left(\sigma^2 + X p_{m,k}^{*(n)} \bar{g}_{m,k}^{(n)}\right)}{g_{i,k}^{(n)}}$, in case of $o_{mk}^{*(n)} = 1$

V. Numerical Results and Performance Analysis

In this section, numerical results are presented and we analyze the performance of the designed energy efficient resource management scheme in detail for this machinery network.

A. Experimental Preparations

In this simulation, there are 4 UAVs originally deployed at the vertexes of an 800×800 m^2 square area and flying in a straight route between the opposite vertexes. We consider that the working speed of the UAVs is 40m/s and their flying altitude is fixed at 20m. MAs are distributed randomly in this range, in which those are served via either U2M or EH-M2M transmissions within a time slot. Moreover, it is considered that the distance between EH-M2M pairs is in the range of (20, 50) m. Denote $\lambda = 3$mJoule/s as the rate of Poisson Process followed by the EH model. We set the uniform distribution between [0, 100] for the sum energy enabling to be harvested. In the simulation experiment, each configuration generates 100 independent runs and averages the performance of EE by using PC Intel® Core (TM) i7–8700 CPU @ 3.2 GHz with MATLAB R2018a. For the purpose of validating the effectiveness of the designed scheme, we propose a set of comparisons with the other four schemes: (1) The scheme maximizes EE without EH considered (non-EH); (2) The scheme maximizes EE with equally separating each time slot into EH time and transmission time (EH-T); (3) The scheme maximizes the transmission rate (max-TR); (4) The scheme maximizes the spectrum efficiency (max-SE).

Owing to all these schemes adopting iterative algorithm, the convergence speed of the compared schemes is essential, which is influenced by the complexity. In this paper, we assume that the complexity of multiplication or division of a complex number is $O(1)$, and that of addition and subtraction is negligible. Denote the number of loops in steps 9-13 of Algorithm 1 as I_0, the computational complexity of the proposed scheme is given by $I_0O(MN^2K)$, so is that of max-SE, max-TR and non-EH. Additionally, the complexity of EH-T is $O(NK)$. Despite that the proposed scheme did not give the fastest convergence speed due to its computational complexity and full-scale factors considered, it could get the highest average energy efficiency. The reasons for this situation are: (1) as compared to non-EH and EH-T, the proposed scheme takes into account the EH function and EH time in each time slot to make decisions on resource management, which results in a relative lower convergence speed; (2) the proposed scheme is able to acquire the maximum EE since the purpose of the proposed scheme is to maximize EE not like the other schemes, which either totally did not consider EH function or the maximization objects are transmission rate and spectrum efficiency. Moreover,

although the computational complexity of non-EH scheme is the same as that of the proposal et al, it did not take into consideration the EH function of each MA, a crucial issue in our work, and the convergence rate and average EE was lower significantly. The EH-T scheme can obtain a relatively quicker convergence rate since the complexity is lower than that of others.

B. Results and Analysis

After discussing the convergence speed, we analyze the influence of the maximum multiplex factor X on the average EE in Fig. 2. It is apparent that the proposed scheme gets the maximal average EE among five schemes over all conditions. The reason can be deduced that the designed scheme considers both the support of EH function and the optimization of EH time allocation in each time slot, which make a significant contribution to the improvement of energy efficiency. Moreover, there is another significant discovery that the highest average EE can be gained by the time the value of X is set to 3 for all the schemes. The more and less values for X will reduce the energy efficiency. Two reasons for the observation are listed: (1) while the value of X is smaller, the overall network throughput is less accordingly, which might reduce the energy efficiency, and (2) while the X is larger, each U2M channel is reused by more EH-M2M pairs. In such case, more interference will be involved and thus the energy efficiency will be reduced as well. From the result, we deduce that the optimal value for X may be 3 in the proposed scenario. Consequently, we constantly set the value of X to 3 in all the following simulation studies.

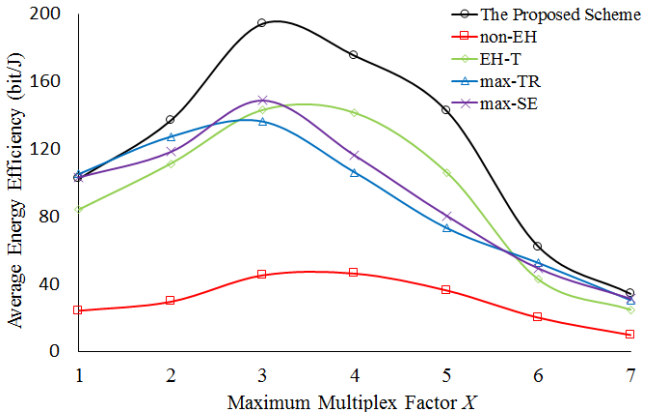

Fig. 2. Average EE versus different values of X

Figs. 3a, 3b and 3c give the demonstration of average EE against the different numbers of deployed MAs with three QoS constraints of minimum required spectrum efficiency (SE=8 *bps/Hz*, SE=12 *bps/Hz* and SE=16 *bps/Hz*) respectively. The reason for setting the minimum required spectrum efficiency at these values is that based on the ITU-R M.2083 specification on spectrum efficiency, the spectrum efficiency for 5G should be about 10 *bps/Hz* [48]. In this simulation, we separately set SE=8 *bps/Hz*, SE=12 *bps/Hz* and SE=16 *bps/Hz* to follow the requirement of 5G network and demonstrate the impacts from different values of minimum required spectrum efficiency on the average EE. It is apparent that the designed scheme acquires the greatest EE among the given schemes throughout most of the conditions. In Fig. 3a and 3b, as the quantity of deployed MA grows, the average energy efficiency follows up initially, for the reason that more MAs will result in increasing the network throughput. Nevertheless, it can

also be seen that by the time the quantity of MAs goes up to 34, the average EE of all schemes tends to be stable until the number further increases to 46. After that, the energy efficiency goes down since the more MAs are deployed, the more mutual interference will be involved, which consumes more transmit power. Interestingly, when the number of MAs further increases to 60, it is worth noting that the average EE will not decrease continuously, and the proposed scheme still gives the best performance among the five schemes in the worst case. The reason for this observation is that although more deployed MAs result in more interference, reducing the energy efficiency in a further way, the distances between transmitter and receiver in MA pairs are shortening, and the shorter transmission distance may improve energy efficiency inversely. In this situation, the energy efficiency may not always decrease. In Fig. 3c, the tendency of average EE versus different numbers of MAs shows a discrepancy against those in Figs. 3a and 3b slightly. With the number of MAs increasing, the average EE shows an upward trend among all the schemes. By the time the quantity of MAs is between 36 and 44, there is a temporary plateau of the energy efficiency, after which time the average EE begins to drop. It is noticeable that the proposed scheme shows an inferior performance than EH-T by the time the quantity of MAs is over 51. When it reaches 62, the average EE remains stable again, while the EH-T achieves the highest performance, next comes the proposed scheme. This is because as the required *SE*=16 *bps/Hz*, more transmit power is needed. Through balancing the EH time and transmission time equally, the system is able to optimize the transmit power. Moreover, it is compared that different values of *SE* can have impacts on the energy efficiency. With the conjunction of Fig. 3a, 3b and 3c, it is clear that the average EE suffers a downward trend while the required *SE* threshold is increasing spanning from 8 *bps/Hz* to 16 *bps/Hz* regardless of which scheme is adopted. When the *SE* goes up to 16 *bps/Hz*, the average EE is approximately half as high as that with 8 *bps/Hz*. The reason is that the smaller minimum required spectrum efficiency means that less transmit power is required, which is able to generate less interference to EH-M2M channels; therefore, the energy efficiency will be better. In addition, it is observed that the non-EH scheme always yields the worst performance of energy efficiency in all cases. Because traditional energy efficient methods consider protecting the resource consumption by bandwidth, power allocation et al; by contrast, EH is regarded as an active way to provide new energy from the outer environment, enhancing the EE in a further way.

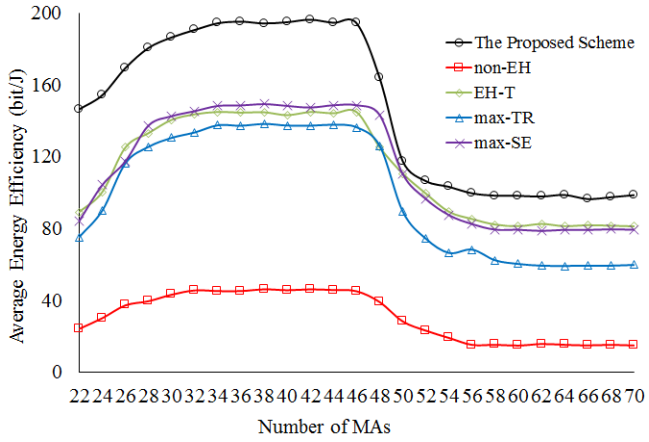

Fig. 3a. Average EE versus different numbers of MAs with $SE = 8\ bps/Hz$

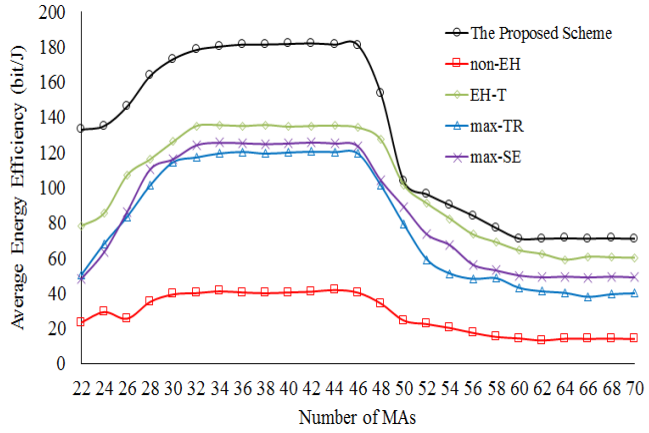

Fig. 3b. Average EE versus different numbers of MAs with $SE = 12\ bps/Hz$

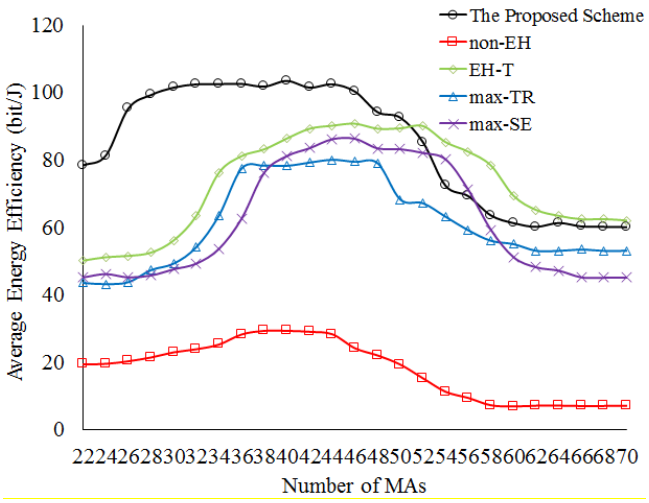

Fig. 3c. Average EE versus different numbers of MAs with $SE = 16\ bps/Hz$

Fig. 4 advances the standard deviation of energy consumption against a different number of placed MAs. The designed scheme can give the optimal performance with an average standard deviation of 29.56, in comparison with 76.08 taking the non-EH scheme, 44.75 taking the EH-T scheme, 37.3 applying the max-TR scheme and 41.84 using the max-SE scheme. The presented observation hinges on the reason that the designed scheme has the capability to stabilize the energy balance for each MA via selecting the optimal EH duration in each time slot, transmit power and available bandwidth to manage the energy consumption to the MAs with more remaining energy. More specifically, from the result, we can also observe that initially there is a rising tendency in the standard deviation when the quantity of MAs goes up, for the reason that at the beginning, the total number of MAs is small and the energy consumption in each MA cannot balance. With an ulterior growth in the quantity of MAs, the standard deviation changes to decline and begins to stabilize until the number of deployed MAs increases to 46. After that, the standard deviation goes up again in that more interference will be involved as the quantity of MAs rises. Moreover, another finding in this simulation declares the standard deviation of consumed energy for the non-EH scheme has gone up drastically in the wake of growing scale of MAs.

The reason is that this scheme manages to transmit power without taking into consideration the available energy residual in each MA.

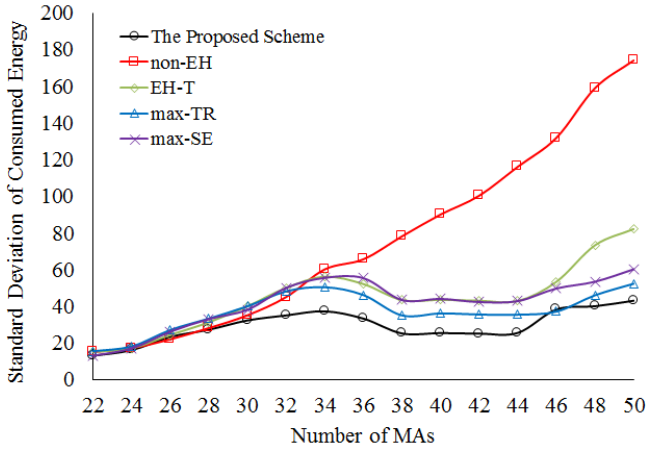

Fig. 4. Standard deviation of consumed energy against different numbers of MAs.

Fig. 5 depicts the EE with varying EH rates λ. From the results, we can discover that the designed scheme has the capability to achieve the highest EE among the five schemes. This is because the designed scheme is able to gain the optimal correlation between EH time and transmission time, which makes a significant contribution to the EE. Furthermore, with the rise of λ, the average EE is enhanced for all schemes except non-EH scheme since there is more energy enabling to be harvested in each time slot in the wake of a higher λ. Whereas, the non-EH scheme gets the least EE and always keeps in constant with the increase of λ in that the non-EH scheme does not take into account the EH function in resource management.

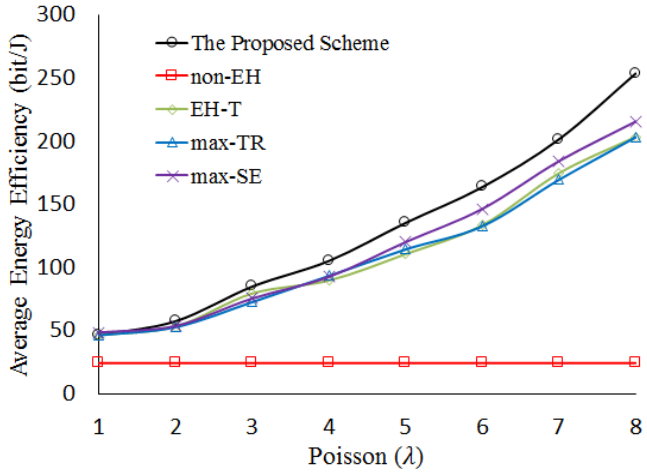

Fig. 5. Average EE versus different energy harvesting rates λ

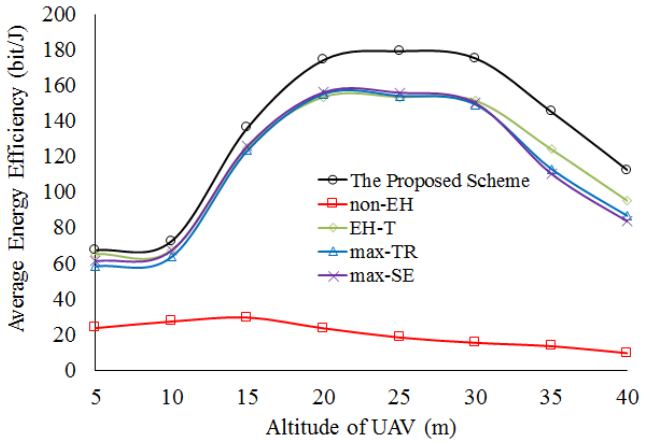

Fig. 6. Average EE versus different altitudes of UAV with the velocity is 40 m/s

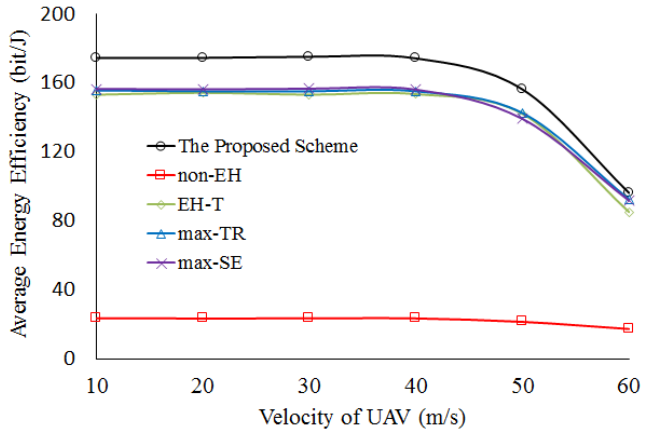

Fig. 7. Average EE versus different velocities of UAV with the altitude is 20 m

Moreover, as the altitude and velocity of UAV are crucial in deciding resource allocation, we conduct extra simulations to illustrate the influence of altitude and velocity of UAVs on the average EE in Fig. 6 and Fig. 7, respectively. Notably, in this study, we set SE=8 *bps/Hz*, the number of MAs is 40, and the value for λ is 3 mJoule/s. From the observation in Fig. 6, we found that the proposed scheme obtains the best performance in varying cases. One important finding is that the highest EE can be achieved by each scheme (except non-EH) when the altitude of UAV ranges from 20 m to 30 m. There are two reasons for this observation: 1) The lower altitude UAV is deployed in, the less sub-bandwidth of UAVs EH-M2M pairs can multiplex, in that the shorter distance results in more interference and most of the MAs are only accessible to the service from UAVs, which consumes more energy; 2) Oppositely, as the altitude of UAV is higher, although more EH-M2M pairs enable to multiplex the sub-bandwidth of UAVs, the long distance between MAs and UAVs will consume more energy as well. Fig. 7 gives the impact of velocity on average EE. It is clear that when the velocity is less than 40 m/s, the EE is constant for all the schemes, which means that the velocity has little effect on EE at the moment. Nevertheless, as the further increase of the velocity, average EE will be reduced since the higher velocity changes the U2M connection frequently, which causes the reduction of transmission rate.

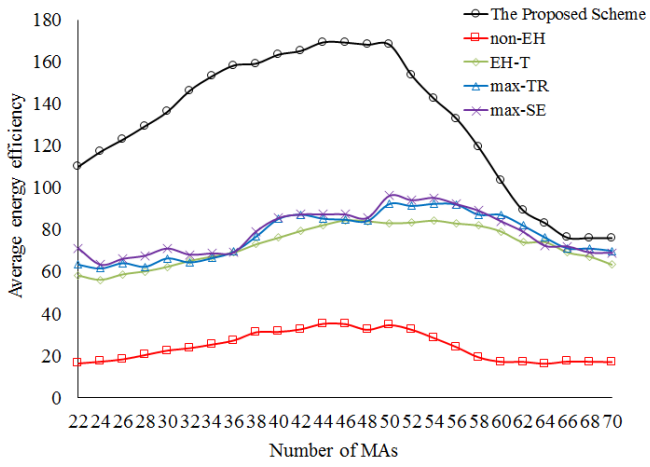

Fig. 8. Average EE with different numbers of MAs in a single terrestrial BS-served scenario

Additionally, in order to illustrate the effectiveness of the UAV-served communications powerfully, we conduct an extra evaluation on average EE for the five schemes in a single terrestrial BS-served and M2M-supported scenario, in which the settings of parameters are the same as those in UAV-served scenario. The value of λ is set to 3 mJoule/s and the constraint for minimum required spectrum efficiency is set to 8 *bps/Hz*. Fig. 8 states the average EE against the quantity of placed MAs in the terrestrial BS-served scenario. Similarly, the designed scheme obtains a more excellent performance than other four schemes as well. While the number of MAs is rising, the average EE witnesses an upward trend among the five schemes with some slight fluctuation, in that more MAs contribute to enlarging the network throughput. Additionally, the fluctuation of tendency derives from the random distribution of ground MAs, causing some slight statistical deviation. The energy efficiency tends to decrease and stabilize at last with the quantity of MAs further going up from 50. Interestingly, in conjunction with Fig. 8 and Fig. 3a, we found that the higher EE can be acquired in UAV-served scenario since the flexible mobility of UAV enables to provide better channel gain to the users, specifically for the edge users in the coverage.

VI. Conclusion

In this paper, we study the energy efficient resource management optimization issue in UAV-served EH-enabled industrial M2M network. To the green characteristics of the proposed network, the optimization problem is jointly considering the EH duration time assignment, transmit power control, bandwidth allocation as well as available energy status of the EH-M2M device with the objective of maximizing the EE and guaranteeing the QoS for all devices concurrently. Since the problem is non-convex and NP-hard, we transform the primitive objective function into a convex form by introducing non-linear fractional programming and variable relaxation method. Moreover, an iterative algorithm on the basis of Dinkelbach and Lagrangian theory is designed to tackle the problem and acquire the optimal resource management strategy. Extensive simulations convincingly demonstrate the effectiveness of the provided method in comparison with the benchmark schemes in various network settings.

APPENDIX A

Denote $EE_{m,n}^{*}$ as the maximum EE of the m-th EH-M2M channel in time slot n. Firstly, if each EH-M2M finds its optimal energy efficiency value $EE_{m,n}^{*}$, the sum energy efficiency of all EH-M2M channels can reach its maximum value as well, in other words the system average energy efficiency has the maximum value EE_{M2M}^{*}. Herein, it can be expressed as (42):

$$EE_{M2M}^{*} = \sum_{n=1}^{N}\sum_{m=1}^{M} EE_{m,n}^{*} \tag{42}$$

Moreover, as we obtain the system average energy efficiency EE_{M2M}^{*}, it is assumed that there is another energy efficiency value $\overline{EE}_{m,n}$ superior to the optimal value $EE_{m,n}^{*}$ in the m-th EH-M2M channel in time slot n. In terms of (42), we define:

$$\overline{EE}_{M2M} = \sum_{n=1}^{N}\left(EE_{1,n}^{*} + EE_{2,n}^{*} + \ldots + \overline{EE}_{m,n} + \ldots + EE_{M,n}^{*}\right) \tag{43}$$

$$EE_{M2M}^{*} = \sum_{n=1}^{N}\left(EE_{1,n}^{*} + EE_{2,n}^{*} + \ldots + EE_{m,n}^{*} + \ldots + EE_{M,n}^{*}\right) \tag{44}$$

On the basis of the assumption $\overline{EE}_{m,n} > EE_{m,n}^{*}$, $\overline{EE}_{M2M} > EE_{m,n}^{*}$ can be deduced, which negatives the aforementioned that EE_{M2M}^{*} is the maximum value. Thus, it is not a true assumption. As the system average energy efficiency EE_{M2M}^{*} is gained, the optimal energy efficiency of each EH-M2M can be acquired as well.

APPENDIX B

In formula (28), the first-order partial derivative for variable $p_{m,k}^{(n)}$ is calculated as (45):

$$\frac{\partial R_{M2M}}{\partial p_{m,k}^{(n)}} = \frac{o_{mk}^{(n)} e_{mk}^{(n)} h_{mk}^{(n)} \sigma^2}{ln\,2\left(e_{mk}^{(n)}\sigma^2 + p_{m,k}^{(n)} \cdot \left(f_{mk}^{(n)} + h_{mk}^{(n)}\right)\right) \cdot \left(e_{mk}^{(n)}\sigma^2 + p_{m,k}^{(n)} f_{mk}^{(n)}\right)} \tag{45}$$

where, $\frac{\partial R_{M2M}}{\partial p_{m,k}^{(n)}}$ can be transformed as (46):

$$\frac{\partial R_{M2M}}{\partial p_{m,k}^{(n)}} = \frac{1}{\left(A + B \cdot p_{m,k}^{(n)}\right) \cdot \left(C + D \cdot p_{m,k}^{(n)}\right)} = \frac{a}{A + B \cdot p_{m,k}^{(n)}} + \frac{b}{C + D \cdot p_{m,k}^{(n)}} \tag{46}$$

in which, $a = \frac{D \pm \sqrt{(D^2 + 4ABCD)}}{2CD}$ and $b = \frac{-2BC}{D \pm \sqrt{D^2 + 4ABCD}}$.

We denote $A = \frac{ln\,2\left(e_{mk}^{(n)}\sigma^2\right)}{o_{mk}^{(n)} e_{mk}^{(n)} h_{mk}^{(n)} \sigma^2}$, $B = \frac{ln\,2\left(f_{mk}^{(n)} + h_{mk}^{(n)}\right)}{o_{mk}^{(n)} e_{mk}^{(n)} h_{mk}^{(n)} \sigma^2}$, $C = \frac{ln\,2\left(e_{mk}^{(n)}\sigma^2\right)}{o_{mk}^{(n)} e_{mk}^{(n)} h_{mk}^{(n)} \sigma^2}$ and $D = \frac{ln\,2\left(f_{mk}^{(n)}\right)}{o_{mk}^{(n)} e_{mk}^{(n)} h_{mk}^{(n)} \sigma^2}$.

In formula (28), the second-order partial derivative for $p_{mk}^{(n)}$, $\frac{\partial R_{M2M}}{\partial p_{m,k}^{2(n)}}$ is a negative value through analyzing (46). Therefore, $R_{M2M}\left(o_{mk}^{(n)}, p_{m,k}^{(n)}\right)$ is concave in $p_{m,k}^{(n)}$.

APPENDIX C

It is knowable that the linear function can be convex and concave. The function $P_{M2M}\left(o_{mk}^{(n)}, p_{m,k}^{(n)}\right)$ is concave in $p_{m,k}^{(n)}$ for the reason that $P_{M2M}\left(o_{mk}^{(n)}, p_{m,k}^{(n)}\right)$ is a linear function for $p_{m,k}^{(n)}$.

APPENDIX D

Since the affine function cannot change the convexity or concavity of the problem. $R_{M2M}\left(o_{mk}^{(n)}, z_{mk}^{(n)}\right)andP_{M2M}\left(o_{mk}^{(n)}, z_{mk}^{(n)}\right)$are affine functions of $R_{M2M}\left(z_{mk}^{(n)}\right)$ and $P_{M2M}\left(z_{mk}^{(n)}\right)$, respectively [49]. It's learned that $R_{M2M}\left(o_{mk}^{(n)}, z_{mk}^{(n)}\right)$ is concave in$o_{mk}^{(n)}$and$z_{mk}^{(n)}$in that$R_{M2M}\left(p_{m,k}^{(n)}\right)$is concave in$p_{m,k}^{(n)}$. Similarly, $P_{M2M}\left(o_{mk}^{(n)}, z_{mk}^{(n)}\right)$ is concave in $o_{mk}^{(n)}$ and $z_{mk}^{(n)}$ in that $P_{M2M}\left(p_{m,k}^{(n)}\right)$ is concave in $p_{m,k}^{(n)}$ as well. Owing to the regulation of constitution [49], the transformed optimization objective function (34) is a convex problem.

REFERENCES

[1] M. Sverko, T. G. Grbac and M. Mikuc, "SCADA Systems With Focus on Continuous Manufacturing and Steel Industry: A Survey on Architectures, Standards, Challenges and Industry 5.0," *IEEE Access*, vol. 10, pp. 109395-109430, 2022.

[2] Z. Zhou *et al*., "Energy-Efficient Resource Allocation for Energy Harvesting-Based Cognitive Machine-to-Machine Communications," *IEEE Transactions on Cognitive Communications and Networking*, vol. 5, no. 3, pp. 595-607, 2019.

[3] M. Li, F. R. Yu, P. Si, E. Sun, Y. Zhang and H. Yao, "Random Access and Virtual Resource Allocation in Software-Defined Cellular Networks With Machine-to-Machine Communications," in IEEE Transactions on Vehicular Technology, vol. 66, no. 7, pp. 6399-6414, July 2017.

[4] Y. -H. Xu, M. Hua, W. Zhou and G. Yu, "Resource Allocation for Cellular Zero-Touch Deterministic Industrial M2M Networks: A Reinforcement Learning-Based Scheme," IEEE Sensors Letters, vol. 6, no. 8, pp. 1-4, 2022.

[5] X. Kuai, X. Yuan, W. Yan and Y. -C. Liang, "Coexistence of Human-Type and Machine-Type Communications in Uplink Massive MIMO," *IEEE Journal on Selected Areas in Communications*, vol. 39, no. 3, pp. 804-819, 2021.

[6] Z. Chang and T. Chen, "Virtual Resource Allocation for Wireless Virtualized Heterogeneous Network With Hybrid Energy Supply," *IEEE Transactions on Wireless Communications*, vol. 21, no. 3, pp. 1886-1896, 2022.

[7] Z. Yang, W. Xu, Y. Pan, C. Pan and M. Chen, "Energy Efficient Resource Allocation in Machine-to-Machine Communications With Multiple Access and Energy Harvesting for IoT," IEEE Internet of Things Journal, vol. 5, no. 1, pp. 229-245, 2018.

[8] N. Tang, S. Mao, Y. Wang and R. M. Nelms, "Solar Power Generation Forecasting With a LASSO-Based Approach," *IEEE Internet of Things Journal*, vol. 5, no. 2, pp. 1090-1099, 2018.

[9] M. -L. Ku, W. Li, Y. Chen and K. J. Ray Liu, "Advances in Energy Harvesting Communications: Past, Present, and Future Challenges," IEEE Communications Surveys & Tutorials, vol. 18, no. 2, pp. 1384-1412, 2016.

[10]C. Zhang, Z. Zhou, P. Liu and B. Gu, "Resource Allocation for Energy Harvesting Based Cognitive Machine-to-Machine Communications," ICC 2019 - 2019 IEEE International Conference on Communications (ICC), 2019, pp. 1-6.

[11]C. Song, S. Liu, G. Han, P. Zeng, H. Yu and Q. Zheng, "Edge Intelligence Based Condition Monitoring of Beam Pumping Units under Heavy Noise in the Industrial Internet of Things for Industry 4.0," *IEEE Internet of Things Journal*.

[12]G. Han, J. Tu, L. Liu, M. Martínez-García and C. Choi, "An Intelligent Signal Processing Data Denoising Method for Control Systems Protection in the Industrial Internet of Things," *IEEE Transactions on Industrial Informatics*, vol. 18, no. 4, pp. 2684-2692, 2022.

[13]H. Wang, G. Ding, F. Gao, J. Chen, J. Wang and L. Wang, "Power Control in UAV-Supported Ultra Dense Networks: Communications, Caching, and Energy Transfer," *IEEE Communications Magazine*, vol. 56, no. 6, pp. 28-34, 2018.

[14]X. Liu, B. Lai, L. Gou, C. Lin and M. Zhou, "Joint Resource Optimization for UAV-Enabled Multichannel Internet of Things Based on Intelligent Fog Computing," IEEE Transactions on Network Science and Engineering, vol. 8, no. 4, pp. 2814-2824, 2021.

[15]W. Mei, Q. Wu and R. Zhang, "Cellular-Connected UAV: Uplink Association, Power Control and Interference Coordination," IEEE Transactions on Wireless Communications, vol. 18, no. 11, pp. 5380-5393, 2019.

[16]Z. Su et al., "Energy Efficiency Optimization for D2D Communications Underlaying UAV-assisted Industrial IoT Networks with SWIPT," IEEE Internet of Things Journal.

[17]H. Wang, J. Wang, G. Ding, J. Chen, Y. Li and Z. Han, "Spectrum Sharing Planning for Full-Duplex UAV Relaying Systems With Underlaid D2D Communications," *IEEE Journal on Selected Areas in Communications*, vol. 36, no. 9, pp. 1986-1999, 2018.

[18]S. Li, Q. Ni, Y. Sun, G. Min and S. Al-Rubaye, "Energy-Efficient Resource Allocation for Industrial Cyber-Physical IoT Systems in 5G Era," IEEE Transactions on Industrial Informatics, vol. 14, no. 6, pp. 2618-2628, 2018.

[19]L. Lyu, C. Chen, S. Zhu and X. Guan, "Resource-Efficient Hierarchical Transmission-Estimation Co-Design for Wireless Control Systems," GLOBECOM 2017 - 2017 IEEE Global Communications Conference, 2017, pp. 1-6.

[20]F. Zhou, L. Feng, M. Kadoch, P. Yu, W. Li and Z. Wang, "Multiagent RL Aided Task Offloading and Resource Management in Wi-Fi 6 and 5G Coexisting Industrial Wireless Environment," IEEE Transactions on Industrial Informatics, vol. 18, no. 5, pp. 2923-2933, 2022.

[21]X. Lu, P. Wang, D. Niyato, D. I. Kim and Z. Han, "Wireless Networks With RF Energy Harvesting: A Contemporary Survey," IEEE Communications Surveys & Tutorials, vol. 17, no. 2, pp. 757-789, 2015.

[22]E. P. C., A. F. G. and R. G., "Energy Harvesting from Machineries for Industries: Vibration as a source of energy," 2020 International Conference on System, Computation, Automation and Networking (ICSCAN), 2020, pp. 1-5.

[23]A. D. Dos Santos, S. C. de Brito, A. V. Martins, F. F. Silva and F. Morais, "Thermoelectric Energy Harvesting on Rotation Machines for Wireless Sensor Network in Industry 4.0," 2021 14th IEEE International Conference on Industry Applications (INDUSCON), 2021, pp. 694-697.

[24]H. Kathiriya, A. Pandya, V. Dubay and A. Bavarva, "State of Art: Energy Efficient Protocols for Self-Powered Wireless Sensor Network in IIoT to Support Industry 4.0," 2020 8th International Conference on Reliability, Infocom Technologies and Optimization (Trends and Future Directions) (ICRITO), 2020, pp. 1311-1314.

[25]S. Kurma, P. K. Sharma, K. Singh, S. Mumtaz and C. -P. Li, "URLLC Based Cooperative Industrial IoT Networks with Non-Linear Energy Harvesting," IEEE Transactions on Industrial Informatics.

[26]G. Cuozzo, C. Buratti and R. Verdone, "A 2.4-GHz LoRa-Based Protocol for Communication and Energy Harvesting on Industry Machines," IEEE Internet of Things Journal, vol. 9, no. 10, pp. 7853-7865, 15 May15, 2022.

[27]P. López Díez, I. Gabilondo, E. Alarcón and F. Moll, "Mechanical Energy Harvesting Taxonomy for Industrial Environments: Application to the Railway Industry," IEEE Transactions on Intelligent Transportation Systems, vol. 21, no. 7, pp. 2696-2706, 2020.

[28]Z. Li, J. Kang, R. Yu, D. Ye, Q. Deng and Y. Zhang, "Consortium Blockchain for Secure Energy Trading in Industrial Internet of Things," IEEE Transactions on Industrial Informatics, vol. 14, no. 8, pp. 3690-3700, 2018.

[29]D. -H. Tran, V. -D. Nguyen, S. Chatzinotas, T. X. Vu and B. Ottersten, "UAV Relay-Assisted Emergency Communications in IoT Networks: Resource Allocation and Trajectory Optimization," IEEE Transactions on Wireless Communications, vol. 21, no. 3, pp. 1621-1637, 2022.

[30]Z. Na, Y. Liu, J. Shi, C. Liu and Z. Gao, "UAV-Supported Clustered NOMA for 6G-Enabled Internet of Things: Trajectory Planning and Resource Allocation," IEEE Internet of Things Journal, vol. 8, no. 20, pp. 15041-15048, 2021.

[31]Y. Yu, J. Tang, J. Huang, X. Zhang, D. K. C. So and K. -K. Wong, "Multi-Objective Optimization for UAV-Assisted Wireless Powered IoT Networks Based on Extended DDPG Algorithm," IEEE Transactions on Communications, vol. 69, no. 9, pp. 6361-6374, 2021.

[32]W. Lu et al., "Trajectory and Resource Optimization in OFDM-Based UAV-Powered IoT Network," in IEEE Transactions on Green Communications and Networking, vol. 5, no. 3, pp. 1259-1270, 2021.

[33]Y. -H. Xu, X. Liu, W. Zhou and G. Yu, "Generative Adversarial LSTM Networks Learning for Resource Allocation in UAV-Served M2M Communications," IEEE Wireless Communications Letters, vol. 10, no. 7, pp. 1601-1605, 2021.

[34]Z. Yao, W. Cheng, W. Zhang and H. Zhang, "Resource Allocation for 5G-UAV-Based Emergency Wireless Communications," IEEE Journal on Selected Areas in Communications, vol. 39, no. 11, pp. 3395-3410, 2021.

[35]X. Liu and N. Ansari, "Resource Allocation in UAV-Assisted M2M Communications for Disaster Rescue," IEEE Wireless Communications Letters, vol. 8, no. 2, pp. 580-583, 2019.

[36]J. Cui, Y. Liu and A. Nallanathan, "Multi-Agent Reinforcement Learning-Based Resource Allocation for UAV Networks," IEEE Transactions on Wireless Communications, vol. 19, no. 2, pp. 729-743, 2020.

[37]Y. Xu, Z. Liu, C. Huang and C. Yuen, "Robust Resource Allocation Algorithm for Energy-Harvesting-Based D2D Communication Underlaying UAV-Assisted Networks," IEEE Internet of Things Journal, vol. 8, no. 23, pp. 17161-17171, 2021.

[38]Z. Yang, W. Xu and M. Shikh-Bahaei, "Energy Efficient UAV Communication With Energy Harvesting," in IEEE Transactions on Vehicular Technology, vol. 69, no. 2, pp. 1913-1927, 2020.

[39]B. Ji, Y. Li, B. Zhou, C. Li, K. Song and H. Wen, "Performance Analysis of UAV Relay Assisted IoT Communication Network Enhanced With Energy Harvesting," in IEEE Access, vol. 7, pp. 38738-38747, 2019.

[40]C. -C. Lai, L. -C. Wang and Z. Han, "The Coverage Overlapping Problem of Serving Arbitrary Crowds in 3D Drone Cellular Networks," *IEEE Transactions on Mobile Computing*, vol. 21, no. 3, pp. 1124-1141, 2022.

[41]M. Monwar, O. Semiari and W. Saad, "Optimized Path Planning for Inspection by Unmanned Aerial Vehicles Swarm with Energy Constraints," *2018 IEEE Global Communications Conference (GLOBECOM)*, 2018, pp. 1-6.

[42]H. Yang, J. Zhao, Z. Xiong, K. -Y. Lam, S. Sun and L. Xiao, "Privacy-Preserving Federated Learning for UAV-Enabled Networks: Learning-Based Joint Scheduling and Resource Management," *IEEE Journal on Selected Areas in Communications*, vol. 39, no. 10, pp. 3144-3159, 2021.

[43]M. M. Sandhu, S. Khalifa, R. Jurdak and M. Portmann, "Task Scheduling for Energy-Harvesting-Based IoT: A Survey and Critical Analysis," *IEEE Internet of Things Journal*, vol. 8, no. 18, pp. 13825-13848, 2021.

[44]Y. Cheng, J. Zhang, J. Zhang, H. Zhao, L. Yang and H. Zhu, "Small-Cell Sleeping and Association for Energy-Harvesting-Aided Cellular IoT With Full-Duplex Self-Backhauls: A Game-Theoretic Approach," *IEEE Internet of Things Journal*, vol. 9, no. 3, pp. 2304-2318, 2022.

[45]K. W. Choi, L. Ginting, P. A. Rosyady, A. A. Aziz and D. I. Kim, "Wireless-Powered Sensor Networks: How to Realize," *IEEE Transactions on Wireless Communications*, vol. 16, no. 1, pp. 221-234, 2017.

[46]J. Tan, Y. -C. Liang, L. Zhang and G. Feng, "Deep Reinforcement Learning for Joint Channel Selection and Power Control in D2D Networks," IEEE Transactions on Wireless Communications, vol. 20, no. 2, pp. 1363-1378, 2021.

[47]W. Dinkelbach, "On nonlinear fractional programming," Management Science, vol. 13, no. 7, pp. 492–498, 1967.

[48]ITU-R M.2083, IMT Vision – "Framework and overall objectives of the future development of IMT for 2020 and beyond", Sep. 2015.

[49]S. Boyd and L. Vandenberghe, *Convex Optimization.* Cambridge University Press, 2004.